Structural Changes of Silk Fibers Induced by Heat Treatment

MASUHIRO TSUKADA,[1]* GIULIANO FREDDI,[2] MASANOBU NAGURA,[3] HIROSHI ISHIKAWA,[3] and NOBUTAMI KASAI[4]

[1]National Institute of Sericultural and Entomological Science, Tsukuba City, Ibaraki 305, Japan, [2]Stazione Sperimentale per la Seta, via G. Colombo 81, 20133 Milano, Italy, [3]Faculty of Textile Science and Technology, Shinshu University, Ueda, Nagano 386, Japan, and [4]Department of Applied Chemistry, Faculty of Engineering, Osaka University, Yamadaoka, Osaka 565, Japan

SYNOPSIS

The structural changes of silk fibers induced by heat treatment were investigated by thermomechanical analysis, dynamic mechanical measurements, X-ray diffraction analysis, and refractive indices measurements. *Bombyx mori* silk fibers exhibited only a slight contraction, while tussah silk fibers showed a prominent two-step contraction during the heating process. The dynamic storage modulus of *B. mori* fibers remained unchanged until the final decrease at about 170°C. The E' value of tussah fibers showed a slight increase ranging from 30 to 70°C and a final abrupt decrease at about 190°C. The broad peak of dynamic loss modulus showed a maximum at 220 and 230°C for *B. mori* and tussah silk fibers, respectively. The crystalline structure of silk fibers did not show any significant change regardless of heat treatment. The birefringence value of *B. mori* silk remained unchanged in the range from 25 to 240°C and then decreased, while that of tussah fibers decreased linearly. The isotropic refractive index increased for both silk fibers, even though with a different rate with increasing temperature. We proposed a schematic representation showing the structural changes of silk fibers induced by heat treatment, taking into account the changes in molecular orientation in the amorphous, laterally ordered and crystalline regions.

INTRODUCTION

In recent years there has been a considerable interest in silk fibroins, naturally occurring high-molecular-weight fibrous protein produced by different species of silkworms. The structure of silk proteins has been extensively studied either in liquid and solid state. Recently, the interest in silk fibroin morphology and structure increased due to its attractiveness for bio-related applications. For example, silk has been used as substrate for enzyme immobilization.[1,2] It has been also pointed out that silk fibroin is presently being tested as blood compatible material.[3] In addition, the more complete understanding of silk structure provided the possibility of exploiting silk fibroin for new uses, such as the production of oxygen-permeable membranes[4,5] and biocompatible materials for medical applications, besides the traditional use as a textile fiber.

In our previous studies,[6-11] we have elucidated the physicochemical properties of protein fibers either grafted with vinyl monomers or chemically modified with epoxides and dibasic acid anhydrides. It appeared that the graft copolymerization and chemical modification techniques are interesting from the point of view of their application, since these chemical agents reacted with the active sites in the amorphous regions of silk fibroin and improved the morphological and structural properties of the fibers.

Among the wide variety of silks, the fibrous materials produced by the *Bombyx mori* (domestic) and *Antheraea, Philosamia,* etc. (wild) silkworms are undoubtedly the most important and have been the subject of several studies. It is noteworthy to point out that the content of only two amino acid residues (glycine and alanine) comprises about 70% of the silk fibroins, either in domestic or wild silk fibers.[12] However, the relative amount of glycine is higher

* To whom correspondence should be addressed.

Journal of Applied Polymer Science, Vol. 46, 1945–1953 (1992)
 CCC 0021-8995/92/111945-09

in the former than in the latter. Moreover, the wild silk fibroins show a larger amount of basic and acidic amino acid residues reactive toward chemical agents.[13,14] The amino acid composition and sequence greatly influence the conformation of *B. mori* and wild silk fibroins in liquid state. The presence of α-helical portions consisting of $-(Ala)_n-$ sequences has been confirmed in the liquid silk fibroin from *Philosamia cynthia ricini* by ^{13}C-NMR analysis.[15] The molecules of *B. mori* silk fibroin take a random coil conformation in dilute aqueous solutions, even though the content of helical structure increase dramatically at concentration higher than 5%.[16] It has been established that the structure and conformation of silk fibroin in the solid state depend strongly on the conditions of sample preparation.[17,18] Loose helix Silk I,[19] antiparallel β-sheet (Silk II)[20,21] as well as random coil conformations have been proposed for silk fibroin. From X-ray diffraction studies, the antiparallel β-sheet structure has been identified as the predominant crystalline modification of either *B. mori* or wild silk fibers. The crystalline regions of the former contain several repetitions of the basic sequence $-(Gly-Ala-Gly-X)_n-$,[22] with X = Ser or Tyr, while those of the latter are mainly of the type $-(Ala)_n-$.[23] On the other hand, the amorphous regions contain most of the amino acid residues with bulky and polar side chains, which are more abundant in wild silk fibroins.

The physical and mechanical properties as well as the chemical reactivity[13,14] of silk fibers have been elucidated in relation to their chemical composition and to the molecular structure of amorphous and crystalline regions.

Silk fibers undergo several kinds of heat treatments, either in dry or wet state, in the course of textile processing. The heat treatments sometimes result in changes in the structure of amorphous and crystalline regions. However, only little attention has been paid to study the structural changes induced by the heat treatments. The knowledge of their effects might contribute to improve the processing conditions as well as to give the hint for producing limited modifications of the fiber characteristics in order to improve their textile performances, such as dyeability, mechanical behavior, handling, etc., and to expand their use for new applications. Thus, the comparative investigation of the changes in the fine structure of various kinds of silk fibers induced by heat treatment entails either foundamental or applied interests in relation to the technological problems of silk production.

The main purpose of this work is a comparison of the physical properties of silk from two different species. The present study was also undertaken in order to elucidate the fine structural changes, i.e., the molecular conformation, crystallinity, and molecular orientation either in the amorphous or crystalline regions as a function of heat treatment on different kinds of silk fibers from *B. mori* and *Antheraea pernyi* silkworms. The modification of silk fiber structure was investigated by thermomechanical analysis, dynamic mechanical measurements, X-ray diffraction analysis, and refractive indices measurements. A newly proposed schematic model representing the structural changes in the crystalline, laterally ordered, and amorphous regions of silk fibers will be discussed in relation to the effect of the heat treatments.

EXPERIMENTAL

Materials

Raw silk fibers were obtained after reeling of cocoon fibers of the silkworm variety *B. mori* (domestic silkworm) or *A. pernyi* (wild silkworm). *B. mori* silk fibers were degummed with an aqueous solution of soap (0.5%) at boiling (98°C) for 1 h. The tussah silk fibers were degummed by conventional method using sodium carbonate–sodium silicate mixture system and thus the samples were prepared.

Silk fiber samples sealed in an aluminum pan were preliminary heat-treated in the differential scanning calorimeter furnace in N_2 gas atmosphere, starting from room temperature to the required temperature at the heating rate of 10°C/min.

Measurements

A Rigaku Denki model CN-8361 apparatus for thermomechanical analysis (TMA) was used to detect the thermal expansion and contraction properties in the course of the heating process. The heating rate was 10°C/min, and sweep dry N_2 gas provided the inert atmosphere. TMA full scale was ± 500 μm. The initial load applied to the sample was 1 g. All the measurements were repeated for reproducibility.

Dynamic mechanical properties were measured using a Toyoseiki Rheolograph Solid-S. The frequency of oscillation was adjusted to be 10 Hz. The temperature range studied was from -10 to 270°C, and the samples were heated at 2°C/min. The dynamic mechanical properties of silk fibers in water were determined with the same apparatus equipped with a home-made accessory especially designed for this purpose.

The X-ray diffraction intensity curves were obtained at a scanning rate of 1°/min, time constant of 1 s, scanning region of 5–35°, counter range of 1K X2 with a diffractometer (Rigaku Denki Co., Ltd.) with CuK_α radiation (λ = 1.54 Å). The voltage and current of the X-ray source were 40 kV and 20 mA, respectively.

The refractive indices, either parallel ($n_{\parallel}$) or perpendicular to the fiber axis ($n_{\perp}$), were measured with the Becke's line method using a polarized microscope under the monochromatic light (Na light) at 20°C and 65% relative humidity (RH). The conditions for the measurements have been described in detail elsewhere.[24]

RESULTS AND DISCUSSION

Thermomechanical Behavior

Figure 1 shows the thermal expansion and contraction properties of silk fibers measured by thermomechanical analysis (TMA). In the range from room temperature to 120°C, the *B. mori* fiber (a) exhibited a slight contraction of about 0.7%, which may be attributed to the evaporation of humidity absorbed by the specimen. The length of the fiber remained almost unchanged at above 120°C and then started to extend slightly at a constant rate from 170°C upward. The *B. mori* silk fiber showed a predominant abrupt extension at around 310°C, due to the breaking and reforming of the interchain hydrogen bonds and to the partial thermal decomposition. The position of the final extension is in accord with the decomposition temperature of the fiber with β' molecular configuration.[25] It is interesting to note that the TMA thermograms (Fig. 1) are similar to the differential scanning calorimetry (DSC) curves[6] in the range from room temperature to about 300°C. Both measurements show only marginal thermal changes, giving evidence of the thermal stability of *B. mori* silk fibers. The tussah silk fibers (b) showed a prominent two-step contraction in the temperature range from 25 to 250°C. The first step appeared in the range from 25 to about 100°C and could be related to the evaporation of the water absorbed by the fiber. The second step started at above 200°C, accompanied by the abrupt change of slope of the TMA curve, and attained a maximum at 250–260°C. The tussah silk fibers begun to extend quite rapidly at above 260°C, even though at an ununiform rate (see the slope change at about 300°C). The final abrupt extension occurred at about 340°C, 30°C higher than *B. mori* silk fibers, as expected from the fact that tussah silk decomposes at higher temperature,[26] due to the thermal stability[27] of the $-(Ala)_n-$ sequences forming the crystalline regions.

The maximum amount of contraction exhibited by tussah silk fibers in the heating process was 3.6%,

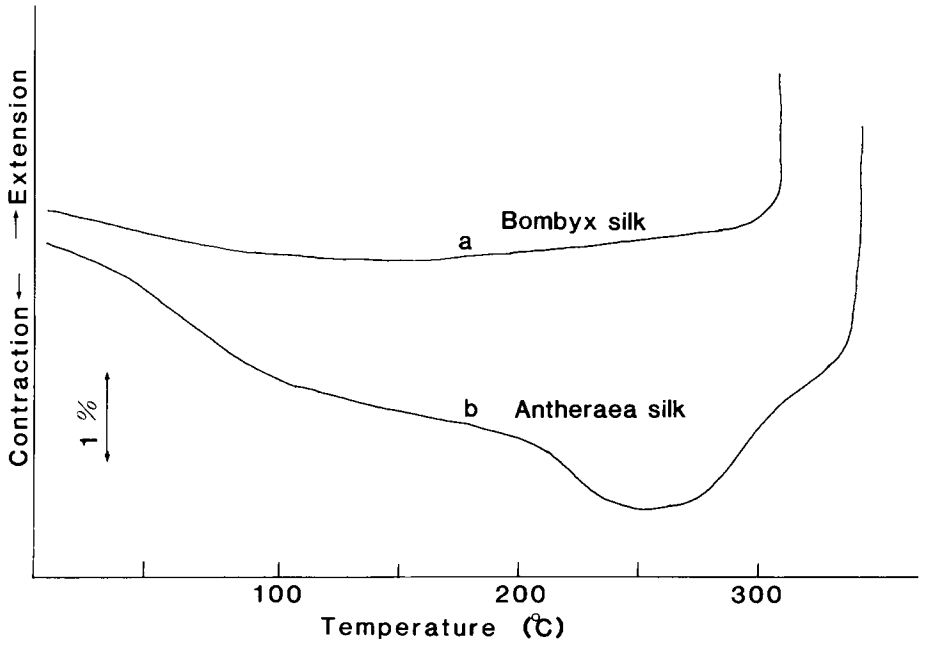

Figure 1 Thermomechanical analysis curves of (a) *B. mori* and (b) *A. pernyi* (tussah) silk fiber.

more than 5 times higher than that of *B. mori* fibers. These results of silk fibers are in good agreement with the microscopic observations of fine structural features. From the point of view of the fiber texture, tussah silk fibers are characterized by a high porosity.[28] In fact, the presence of several vacuolar droplets of different shape and size (from 0.2 to 1.3 μm) was observed by comparative ultrastructural observations of cocoon filaments,[24] while *B. mori* fibers did not show any evidence of this feature. Moreover, the density of tussah silk fibers measured in CCl_4 is markedly lower than that of *B. mori* fibers.[28] It has been recently shown by DSC analysis that tussah silk fibers undergo some thermal transitions in the range from 200 to 300°C, before their decomposition.[17,18] Even though these intrinsic thermal behaviors have not been clearly elucidated yet, they appeared to be related to conformational changes occurring in the amorphous regions of the fiber in the course of the heating process. Moreover, we reported[24] that tussah silk fibers treated with epoxides exhibited a rather different thermal behavior, suggesting that the thermal transitions in the range from 200 to 300°C are mainly related to the arrangement of fibroin molecules in the amorphous regions.

Dynamic Mechanical Behavior

In order to elucidate the structural changes of silk fibers during the heating process, we investigated the temperature dependence of the dynamic mechanical properties either in dry or wet state. Figure 2 shows the dynamic storage (E') and loss (E'') moduli curves of *B. mori* silk fibers in standard state (20°C, 65% RH). The E' value showed a slight decrease in the range from −10 to 10°C and then remained almost unchanged as the temperature increased up to 150°C. The thermal movement of fibroin molecules became evident at above 150°C and the E' value decreased rapidly at about 170°C. The loss modulus (E'') curve did not show any significant change until 170°C, at which temperature the broad E'' peak begun to appear, exhibiting a maximum at 220°C. The temperature dependences of storage (E') and loss (E'') moduli of tussah silk fibers are shown in Figure 3. The E' curve showed a minimum at around 15–20°C, then increased quite sensibly reaching a plateau at 70°C. No other changes were detected until 190°C, at which temperature the E' value rapidly decreased, as a consequence of the higher thermal movement of fibroin chains attributed to the weakening of the intermolecular interactions. The loss modulus (E'') curve exhibited a single broad peak starting at about 190°C with a maximum at 230°C, 10°C higher than *B. mori* silk fibers.

It is interesting to note that the positive inflection of the E' curve of tussah silk fibers ranging from 30 to 70°C corresponds to their significant contraction determined by thermomechanical analysis (Fig. 1). These findings suggest that there should have been some rearrangements of the tussah fibroin molecules in the amorphous regions[24] during the heating process, resulting in a strengthening of the interchain interactions. *B. mori* fibers did not show this behavior and their thermal stability below 100°C should be partly attributed to the higher degree of molecular orientation even in the amorphous regions as well as to the more compact fibrous structure.

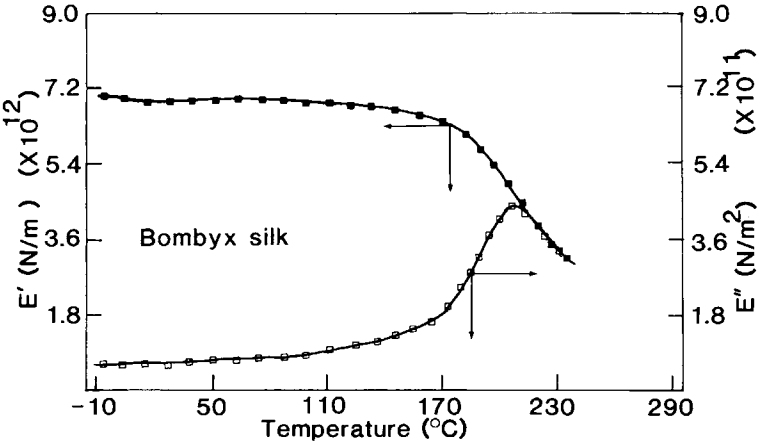

Figure 2 Plots of the dynamic mechanical storage modulus (E') (■) and the dynamic mechanical loss modulus (E'') (□) for the *B. mori* silk fiber.

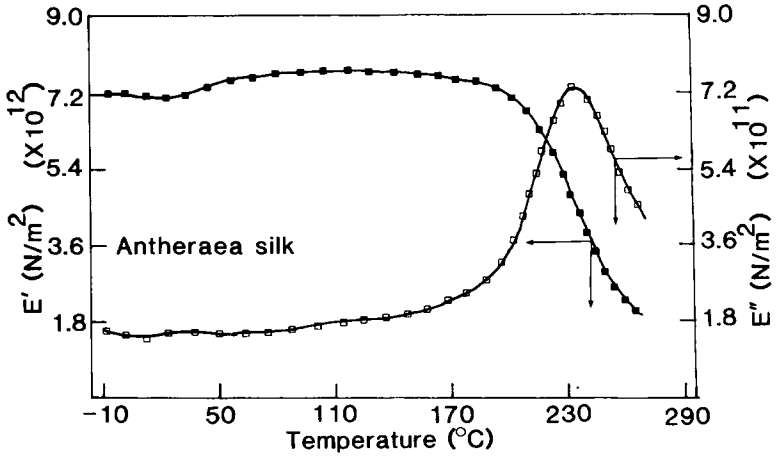

Figure 3 Plots of the dynamic mechanical storage modulus (E') (■) and the dynamic mechanical loss modulus (E'') (□) for the *A. pernyi* silk fiber.

It has been shown that the glass transition temperature of *B. mori* silk fibroin membranes is located at around 175°C,[29] on the basis of TMA measurements. This temperature corresponds to the abrupt negative inflection of E' curve. Assuming that the general thermal behavior of tussah silk fibers is quite similar to that of *B. mori* silk, we can suggest that the glass transition temperature is located at around 190°C.

The E'' peak appearing at 230°C in tussah silk fibers has been attributed to the molecular motion in the crystalline regions because the spacings corresponding to the intersheet distance gradually expand at above 190°C[26] at which temperature the E'' peak begins (Fig. 3). The higher peak temperature for tussah silk fibers is in agreement with the results of TMA and DSC measurements[24,26] and gives evidence of the thermal stability of the $-(Ala)_n-$ sequences[27] in the crystalline regions.

The behavior of the dynamic storage modulus (E') has been measured with silk fibers immersed in water at different temperatures from 10 to 60°C (Fig. 4). The E' value of both *B. mori* (a) and tussah silk fibers (b) decreased with increasing the temperature, even though the rate and extent of E' lowering were markedly higher for tussah silk fibers.

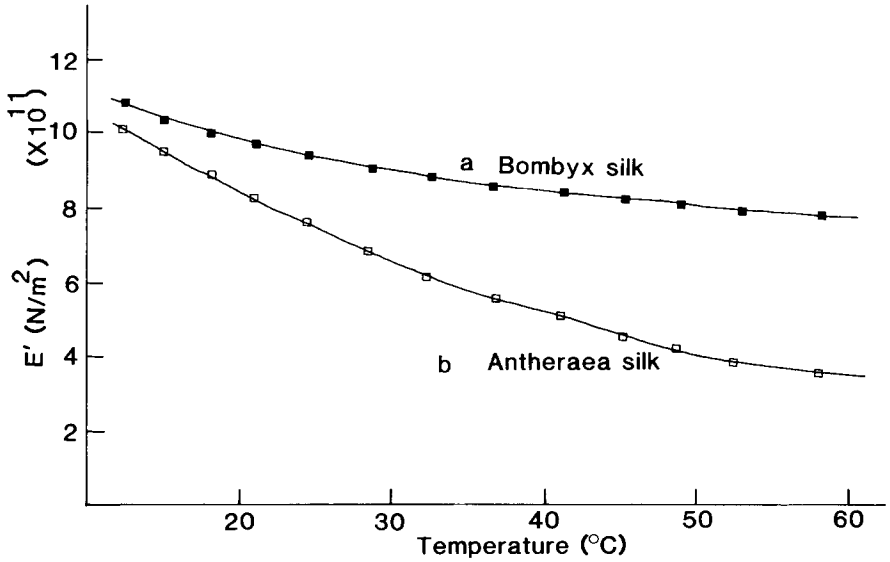

Figure 4 Plots of the dynamic mechanical storage modulus (E') for the *B. mori* (■) and *A. pernyi* (□) silk fibers in the water measured in the course of the heating process.

The effect of water absorption is the fiber swelling due to the penetration of water molecules in the more accessible, noncrystalline regions. Interchain crosslinks tend to be broken and replaced by hydrogen bonds with water. The insertion of one or a few layers of water molecules between adjacent fibroin chains should weaken their mutual interactions and their mobility should increase during the heating process. The viscoelastic properties of silk fibers in wet state could be related to the structure of their amorphous regions, because in the experimental conditions adopted, the closely packed crystalline regions were not affected. Therefore, we can elucidate that the amorphous regions of *B. mori* silk fibers should possess a higher degree of order and molecular orientation compared to tussah fibers: Even though the direct interchain interactions are weakened by the penetration of water, the fibroin chains are hindered from moving as freely as those of tussah silk fibers.

Crystalline Structure

In order to elucidate whether the thermal treatments affected the crystalline structure, X-ray diffraction curves of silk fibroin fibers were analyzed at high temperatures ranging from 200 to 260°C. The crystalline structure of *B. mori* silk fibers remained unchanged regardless of the heat treatment (X-ray diffraction curves not reported). Figure 5 shows the

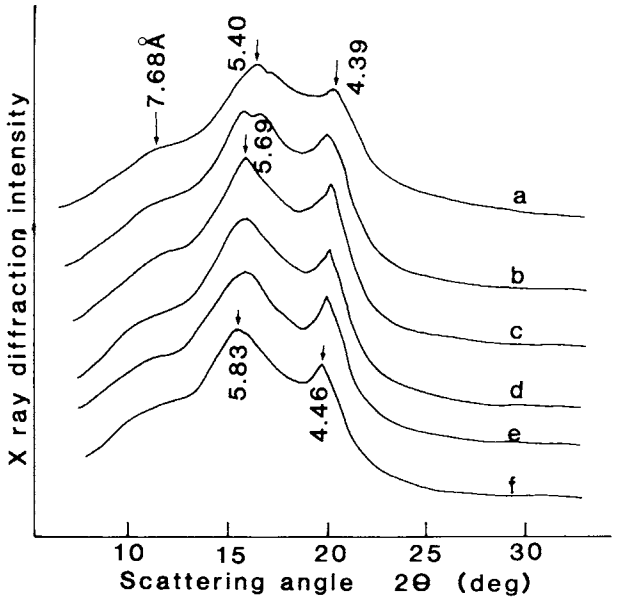

Figure 5 Diffraction patterns of the tussah silk fibers recorded at different elevated temperatures. Temperature (°C): (a) 25, (b) 200, (c) 215, (d) 230, (e) 245, (f) 260.

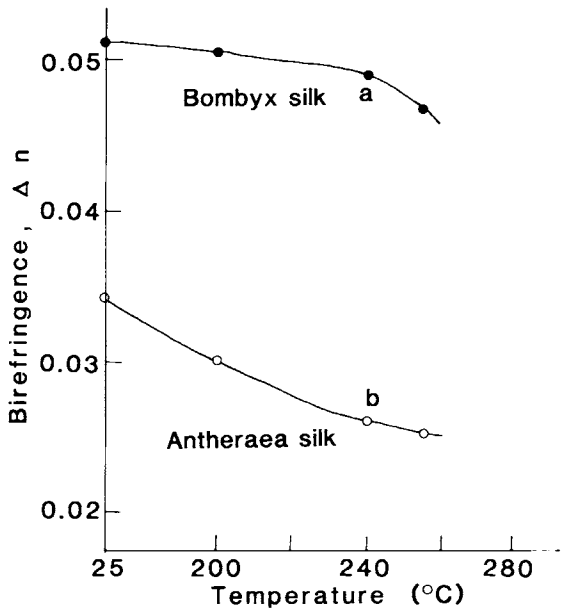

Figure 6 Birefringence of the (a) *B. mori* (●) and (b) *A. pernyi* (○) silk fibers preliminary heat-treated at different temperatures.

X-ray diffraction curves of tussah silk fibers at 25°C (control sample, a) and at elevated temperatures [(b)–(f)]. The reference sample (a) showed diffraction peaks corresponding to the spacings of 7.68, 5.40, and 4.39 Å, attributed to the β-crystalline structure of silk fibroin.[26] The X-ray diffraction peaks corresponding to these spacings shifted slightly to smaller angles when the measurement was carried out at above 230°C. This shift could be attributed to the slight increase of the intersheet spacings of the β crystals and is in agreement with the results already reported.[26] These findings coincide with the observation that the intersheet distance of β crystals expands gradually at above 190°C.[26] Nevertheless, from our results, we can infer that the crystalline structure of tussah silk fibroin fibers was not significantly affected by the thermal treatment and remained essentially unchanged.

Refractive Indices

In order to elucidate the structural changes induced by heat treatment, we determined the birefringence (Δn) of silk fibers heat-treated at different temperatures. Birefringence may be regarded as a measure of the average orientation of the molecules in a fibrous polymer. Figure 6 shows that the birefringence of *B. mori* silk fibers (a) did not change noticeably regardless of the heat treatment in the range from 25 to 240°C. As the temperature exceeded 240°C,

the Δn value showed a slight decrease evidentiated by the negative inflection of the curve. However, it is interesting to note that tussah silk fibers (b) exhibited a markedly lower birefringence value at 25°C, suggesting their poor intrinsic molecular orientation compared to *B. mori* fibers. Moreover, the degree of orientation of tussah silk decreased linearly in relation to the treatment temperature.

Figure 7 shows the isotropic refractive index (n_{iso}) in relation to the treatment temperature. *B. mori* silk fibers (a) exhibited a linear increase of the n_{iso} value in the temperature range examined. The n_{iso} value of tussah silk fibers increased, but the rate and extent was quite different. The n_{iso} value markedly increased by heat treatment at 200°C and then exhibited the tendency to saturate at above 200°C. The isotropic refractive index is related to the crystallinity of the fiber.[30] According to the results of X-ray analysis, it has been shown that the crystalline regions of both *B. mori* and tussah silk fibers have not been directly affected by the thermal treatment. Therefore, we should estimate that the variations of refractive indices (Figs. 6 and 7) were due to some changes that occurred in the less-ordered regions of the silk fibers.

DISCUSSION

From the preceding results it seems that the less-ordered amorphous regions play the major role in determining the behavior of silk fibers subjected to heat treatment. Furthermore, we suppose that the differences in fine structure between *B. mori* and

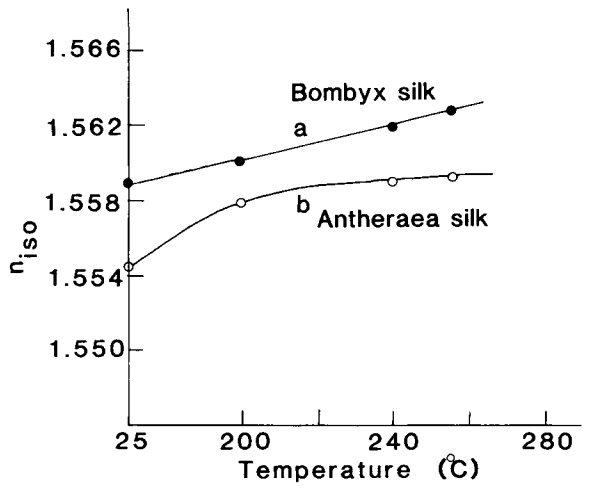

Figure 7 Isotropic refractive index (n_{iso}) of the (a) *B. mori* (●) and (b) *A. pernyi* (○) silk fibers preliminary heat-treated at different temperatures.

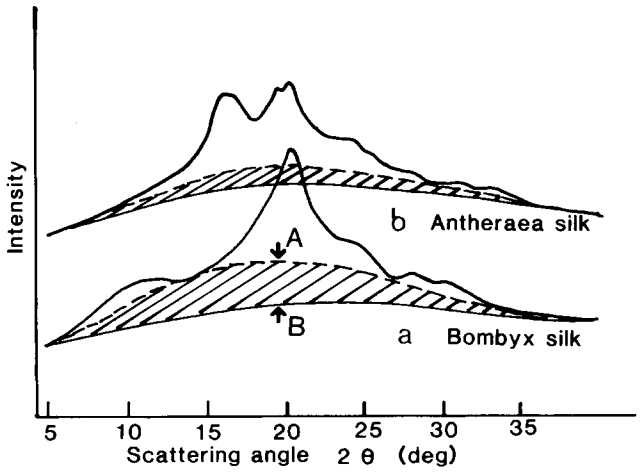

Figure 8 X-ray diffraction curves of the (a) *B. mori* and (b) *A. pernyi* silk fibers. Baseline (A) and (B) are drawn according to the method proposed by Hermans and Weidinger[32] and Sakurada et al.,[33] respectively.

tussah silk fibers should be mainly attributed to the arrangement and to the mutual interactions of the fibroin chains in the amorphous domain of the fiber structure.

Ishikawa[28] investigated the amorphous and crystalline phases of *B. mori* and tussah silk fibers by partial acid hydrolysis. On the basis of the hydrolysis curves and the birefringence values of the unhydrolized residues, he proposed a three-phase model for explaining the fine structure of silk fibroins. Besides the well-packed, highly ordered crystalline regions, identified as the final residue remaining after acid hydrolysis, he presumed the presence of laterally ordered regions as a transition phase between crystalline and amorphous regions. A similar model was suggested by Show,[31] who studied the chemical composition of various fractions obtained from *B. mori* silk fibroin after chymotryptic and tryptic digestion. The fibroin molecules in the laterally ordered regions show a quite high degree of order and orientation, even though they are not well packed as in a perfect crystalline structure. From the hydrolysis kinetics he inferred that the intermediate phase is more abundant in *B. mori* than in tussah silk fibers.

The amorphous regions of an oriented fibrous polymer contribute to the X-ray diffraction profile as a broad background peak. Figure 8 shows the X-ray diffraction curves of *B. mori* (a) and tussah (b) silk fibers. Hermans and Weidinger[32] and Sakurada et al.[33] independently proposed a method for drawing the baseline of the diffraction curve for the calculation of the degree of crystallinity of the fiber. The two methods differ in the way of drawing the baseline

that separates the crystalline from the amorphous contributions to the X-ray diffractogram. The baseline drawn according to the Herman and Weidinger and the Sakurada et al. methods are shown in Figure 8 by a dotted and continuous line, respectively. The percentage of crystallinity calculated according to the Sakurada et al. method is higher than that obtained using the Hermans and Weidinger method. Assuming that the intensity of the broad peak representing the amorphous contribution is proportional to the degree of order and orientation of the amorphous phase, we suggest that the area between the two baselines drawn on the X-ray diffractograms (Fig. 8) as an index representing the laterally ordered regions of the silk fibers.

The fine structural changes induced by thermal treatment on silk fibers can thus be schematically represented by the models shown in Figure 9. The

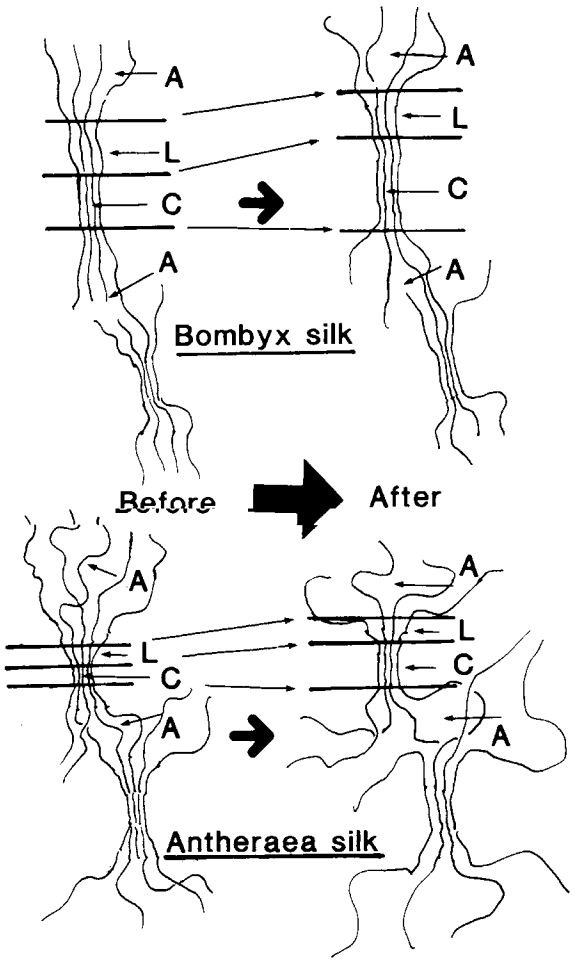

Figure 9 Schematic representation of the structural changes of *B. mori* (upper part) and *A. pernyi* (lower part) silk fibers induced by the heat treatment: L, laterally ordered regions; C, crystalline regions; A, amorphous regions.

number and size of the crystalline regions of *B. mori* silk fibroin increased by heat treatment, due to the close packing of the more adjacent laterally ordered regions, as confirmed by the behavior of the n_{iso} value (Fig. 7) and X-ray diffraction curves (Fig. 8). The low value of contraction observed in *B. mori* silk fibers in the heating process should be attributed to the fact that even in the totally amorphous regions the fibroin chains are not completely free to move, because they are blocked quite firmly in their position. For this reason, the average molecular orientation of *B. mori* silk fibers did not decrease significantly in the heating process as suggested by the Δn values (Fig. 6). These results of refractive indices of tussah silk fibers before and after heat treatment could be attributed to the low contribution of the laterally ordered regions to the thermal stability of the fiber as well as to the intrinsic low degree of order of fibroin chains in the amorphous regions. The number and size of β crystals increased, as in the case of *B. mori* fibroin, but tussah silk fibers exhibited a higher extent of contraction (Fig. 1) produced by the rearrangement of the molecules in the amorphous regions during the heating process and in the preliminary heat treatment, which led to a decrease of the average molecular orientation.

CONCLUSIONS

It was demonstrated that *B. mori* silk fibers exhibited only a slight contraction, while tussah (*A. pernyi*) silk fiber showed a major contraction of 3.5% at 250–260°C, more than 5 times higher to the *B. mori* silk fibers. The original crystalline structure of the *B. mori* silk as well as tussah silk did not show any significant changes in spite of the heat treatment. The birefringence of *B. mori* silk fiber did not change noticeably regardless of the heat treatment, while tussah silk exhibited a markedly lower birefringence when it is heat-treated, implying that the molecular orientation of the amorphous region and not of the crystalline region specifically lowered for tussah silk fiber. Rearrangements of the tussah silk fiber occurred in the amorphous region by the heat treatment because of the lower degree of order and representation. These findings suggest that *B. mori* silks possess the higher degree of order and molecular orientation in the amorphous region, which makes a pronounced contrast with that of tussah silk fibers. These explanations are supported by the experimental results of thermomechanical analysis, dynamic mechanical measurements, and on the basis of the refractive indices data.

This research was partly supported by a special coordination fund for promoting science and technology (STA) in the basic research core system by the Science and Technology Agency.

REFERENCES

1. M. Demura and T. Asakura, *Biotech. Bioeng.*, **33,** 598 (1989).
2. T. Asakura, J. Kanetake, and M. Demura, *Polym.-Plast. Technol. Eng.*, **28,** 453 (1989).
3. H. Sakabe, H. Itoh, T. Miyamoto, Y. Noishiki, and W. S. Hu, *Sen-i Gakkaishi,* **45,** 487 (1989).
4. N. Minoura, M. Tsukada, and M. Nagura, *Polymer,* **31,** 265 (1990).
5. N. Minoura, M. Tsukada, and M. Nagura, *Biomaterials,* **11,** 430 (1990).
6. M. Tsukada, *J. Appl. Polym. Sci. Polym. Phys. Ed.,* **35,** 965 (1988).
7. M. Tsukada, *J. Appl. Polym. Sci. Polym. Phys. Ed.,* **35,** 2133 (1988).
8. M. Tsukada and H. Shiozaki, *J. Seric. Sci. Jpn.,* **58,** 15 (1989).
9. M. Tsukada and H. Shiozaki, *J. Appl. Polym. Sci.,* **37,** 2637 (1989).
10. M. Tsukada and H. Shiozaki, *J. Appl. Polym. Sci.,* **39,** 1289 (1990).
11. M. Tsukada, H. Shiozaki, and A. Konda, *J. Appl. Polym. Sci.,* **41,** 1213 (1990).
12. J. Kirimura, *Bull. Seric. Exp. Station,* **17,** 447 (1962).
13. Y. Tanaka and H. Shiozaki, *Makromol. Chem.,* **129,** 12 (1969).
14. Y. Tanaka and H. Shiozaki, *J. Polym. Sci. Polym. Chem. Ed.,* **12,** 2741 (1974).
15. H. Yoshimizu and T. Asakura, *J. Appl. Polym. Sci.,* **40,** 1745 (1990).
16. Y. Kobayashi, T. Fujiwara, Y. Kyogoku, and K. Kataoka, Abstracts of the 19th Meeting of Nuclear Magnetic Resonance, Japan, 1980, p. 149.
17. M. Tsukada, *J. Appl. Polym. Sci.,* **24,** 457 (1986).
18. M. Tsukada, *J. Appl. Polym. Sci.,* **24,** 1227 (1986).
19. B. Lotz and H. D. Keith, *J. Mol. Biol.,* **61,** 201 (1971).
20. R. D. B. Fraser and T. P. MacRoe, *Conformation in Fibrous Proteins and Related Synthetic Proteins and Related Synthetic Polypeptides,* Academic Press, New York, 1973.
21. M. Shimizu, *Bull. Imp. Sericul. Exp. Sta. Jpn.,* **10,** 441 (1941).
22. F. Lucas, J. T. B. Shaw, and S. G. Smith, *Adv. Prot. Chem.,* **13,** 107 (1958).
23. J. T. B. Shaw and S. G. Smith, *Biochim. Biophys. Acta,* **52,** 305 (1961).
24. M. Tsukada, Y. Gotoh, G. Freddi, M. Matsumura, H. Shiozaki, and H. Ishikawa, *J. Appl. Polym. Sci.,* to appear.
25. H. Ishikawa, M. Tsukada, I. Toizume, A. Konda, and K. Hirabayashi, *Sen-i Gakkaishi,* **28,** 91 (1972).
26. M. Nagura, M. Urushidani, H. Shinohara, and H. Ishikawa, *Kobunshi Ronbunshu,* **35,** 81 (1978).
27. M. Tsukada, M. Nagura, and H. Ishikawa, *J. Polym. Sci. Polym. Phys. Ed.,* **25,** 1325 (1987).
28. H. Ishikawa, H. Sofue, and K. Matsuzaki, *J. Textile Sci. Tech., Shinshu Univ.,* **10,** 176 (1960).
29. J. Magoshi, Y. Magoshi, S. Nakamura, N. Kasai, and M. Kakudo, *J. Polym. Sci. Phys. Ed.,* **15,** 1675 (1977).
30. S. Gladstone and D. Dale, *Phil. Trans.,* **153,** 317 (1863).
31. J. T. B. Show, *Biochem. J.,* **93,** 45 (1964).
32. P. Hermans and H. A. Weidinger, *J. Appl. Phys.,* **19,** 491 (1948).
33. I. Sakurada, K. Nukushina, and N. Mori, *Kobunshi KAGAKU,* **12,** 302 (1955).

Received December 11, 1991
Accepted February 15, 1992